P8R.12 THE USE OF CLEAR-AIR ECHOES FOR OPERATIONAL DOPPLER RADAR SYSTEMS

Kenichi Kusunoki *
Meteorological Research Institute, Tsukuba, Japan

1. INTRODUCTION

Operational C-band Doppler radar systems have been widely used in Japan for meteorological applications. For instance, the Doppler radar for Airport Weather (DRAW) systems as a wind shear detection/warning platform have already been installed at eight major airports. Wind shear detection algorithms that operate on the DRAW are tuned to primarily recognize microbursts and gust fronts, however, the detection of the wind shear in a precipitation free environment has been ignored. It is planned that the weather surveillance radar network in Japan will have a Doppler capability. Radar data assimilation scheme will be run as part of the operational system, therefore, it will become important to monitor pre-storm wind fields within the clear-air boundary layer. This paper discusses the potential of clear-air echoes for operational Doppler radar systems in Japan.

2. METHODOLOGY

The data used in the present study includes the following: (i) the Narita DRAW, (ii) three sites of the Automated Meteorological Data Acquisition System (AMeDAS), and (iii) Aircraft Communications Addressing and Reporting System (ACARS) data from the surface to 3000 m above ground level (AGL) around the Narita International Airport. The locations where the data were taken are shown in Fig. 1. During the study period (from July to December 1997), there were 141 days when clear-air echoes appeared.

3. RESULTS

a. Spatial distribution

Clear-air echo areas observed throughout September 1997 are superimposed in Fig. 2. These figures indicate the distribution of the echoes ending at the coastline, and a distinct contrast was seen between clear-air echoes observed over land and their absence over the ocean.

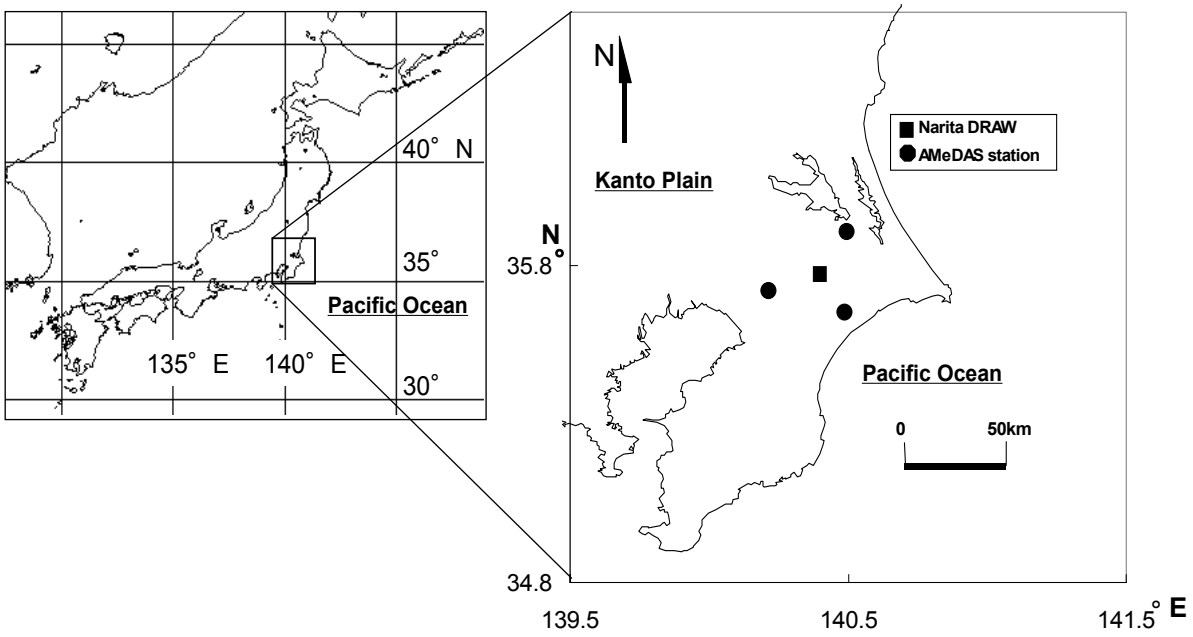

FIG. 1. Map showing the study area. The square indicates the position of the Narita DRAW. Circles indicate the positions of AMeDAS stations.

Corresponding author address:
* Kenichi Kusunoki, Meteorological Research Institute, 1-1,Nagamine, Tsukuba, Japan
E-mail: kkusunok@mri-jma.go.jp

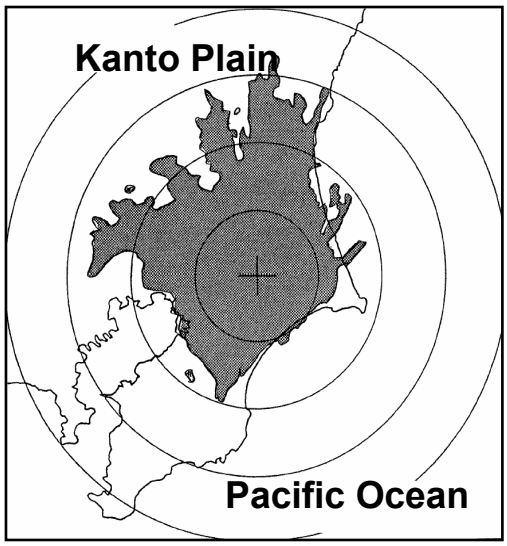

FIG. 2. The example of spatial distribution of clear-air echo appearances (shaded) observed with the Narita DRAW. All clear-air echo areas during September 1997 are superimposed. The location of the Narita DRAW is indicated by the cross. Range marks are at 25-km intervals centered at the Narita DRAW.

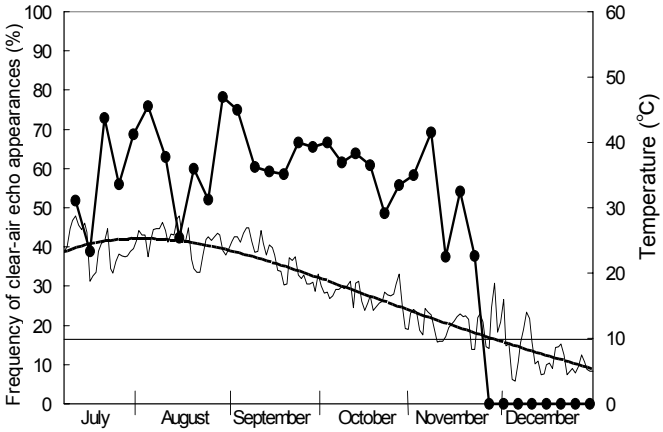

FIG. 3. Seasonal variations of clear-air echo appearances from 1 Jul to 31 Dec. The bold line with circles shows the relative frequency of clear-air echo appearances, which was obtained by dividing total hours of clear-air echo appearances by the no-precipitation period for each 5-day period. The thin line shows the daily average surface temperature from the three AMeDAS sites and the bold curve is the trend.

b. Seasonal variation

Figure 3 indicates the relative frequency of clear-air echo appearances from July to December 1997, where the relative frequency was obtained by dividing total hours of clear-air echo appearances by the no-precipitation period for each 5-day period. During the survey period, the relative frequency varied considerably. From July to late November, clear-air echoes were observed on 40%-80% of no-precipitation days, but clear-air echoes never appeared [i.e., no-echo period, (NEP)] after late November. The drop-off in clear-air echo appearances was associated with the trend in daily average surface temperatures dipping below 10C.

c. Diurnal variation

Figure 4 shows the hourly totals of clear-air echo and no echo for each month. The sunrise and sunset times are also indicated by white and black arrows, respectively, in this figure. The diurnal variation of clear-air echo appearances had two peaks at the periods of the daytime and the twilight. The first peak was in the daytime, starting after sunrise and fading before sunset, while the second one appeared during twilight after sunset for a short time.

d. Relationships of clear-air appearances to surface weather conditions

Figure 5 shows the hourly distribution of surface wind speed in August as the most typical example. This figure indicates that clear-air echoes scarcely appeared where surface wind speeds exceeded 6 ms^{-1}.

e. Relationship between clear-air echo appearances and boundary layer lapse rates

Figure 6 shows the vertical distribution of the relative frequencies of temperature lapse rates from ACARS soundings with no precipitation. The data were analyzed in the period of 0900-1600 JST between July and October, when clear-air echoes appeared almost constantly. Also, in order to remove the effect that clear-air echoes decreased considerably when surface wind speed exceeded 6 ms^{-1}, no echo data were used in the condition of the surface wind speed below 6 m s^{-1}. Figure 6a shows that the relative frequencies are distributed abound 10 K km^{-1} below 1000 m AGL. It is clearly indicated that the lower boundary layers were dominated by well-mixed conditions when clear-air echoes appeared. Figure 6b, in the case that no echo appeared, reveals more stable layers than that for clear-air cases.

4. DISCUSSIONS

The results of this study suggest that clear-air boundary layer is rich in clear-air echoes and operational scan strategies and algorithms for them would be worth developing in Japan. This study also exhibits the unique characteristics of space distribution, diurnal and seasonal variations, and sensitive dependence on boundary layer conditions. These results will be reflected in the limitations and time schedules concerning routine operational use of clear-air echoes. 1) Concerning the spatial distribution, a disadvantage is that clear-air information is not available in the oceanic sector of the radar coverage area because clear-air echoes only appear over land. 2) On the annual schedule for routine monitoring clear-air boundary layers, it is noticeable that the phase is shifted rapidly to no echo period (NEP) when daily average surface temperatures dipping below 10C. During NEP, there is no clear-air echo available for monitoring clear-air circulations. 3) The daily timetable for the use of clear-air echoes should be limited to almost daytime. On the other hand, nighttime boundary layer can be scarcely monitored because of poor/no clear-air echoes. Furthermore, during early morning and evening, Doppler velocity from the echoes may not represent actual wind. 4) Clear-air wind shear detection algorithms may not work accurately due to lack of scatterers under strong wind conditions, because the clear-air echo frequency decreased considerably with surface wind speed exceeding 6ms^{-1}. To obtain reliable information from clear-air echoes, it is necessary to monitor boundary layer conditions such as temperature lapse rates and surface wind speeds, simultaneously with radar observations.

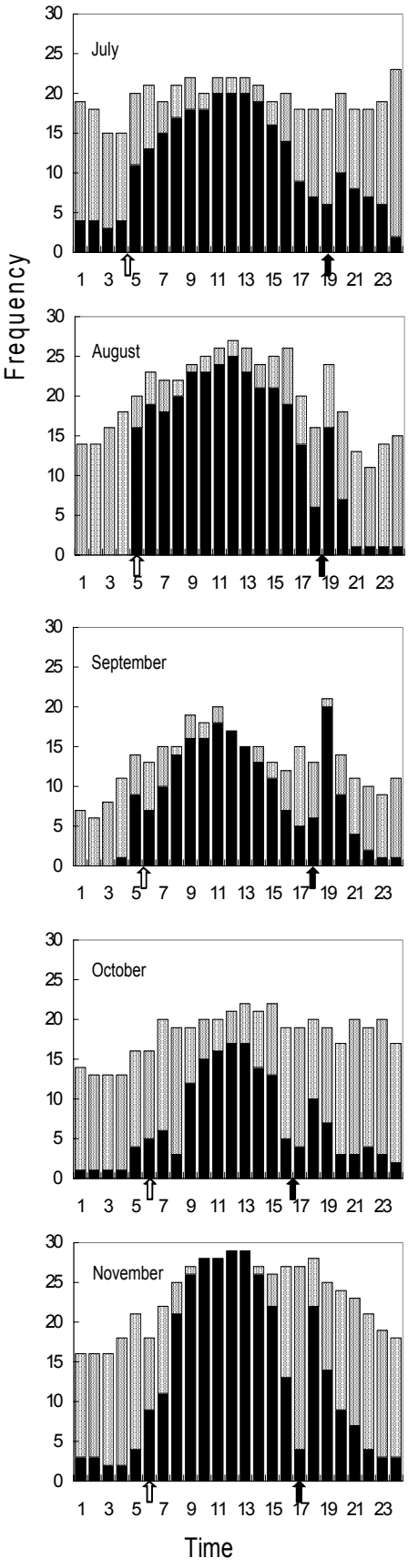

FIG. 4. Diurnal variation of clear-air echo appearances. The black bar shows the hourly totals of “clear-air echo” and the shaded bar those of “no echo” for each month. The white and black arrows show sunrise and sunset times, respectively.

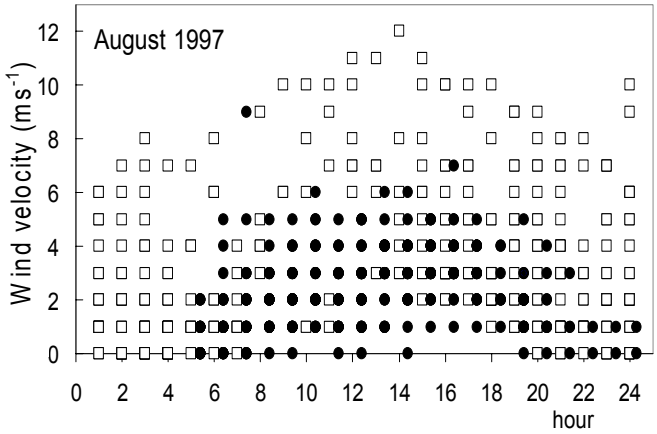

FIG. 5. The hourly distribution of surface wind speed in Aug 1997. Open squares indicate that no echo appeared, while solid circles indicate that clear-air echo appeared.

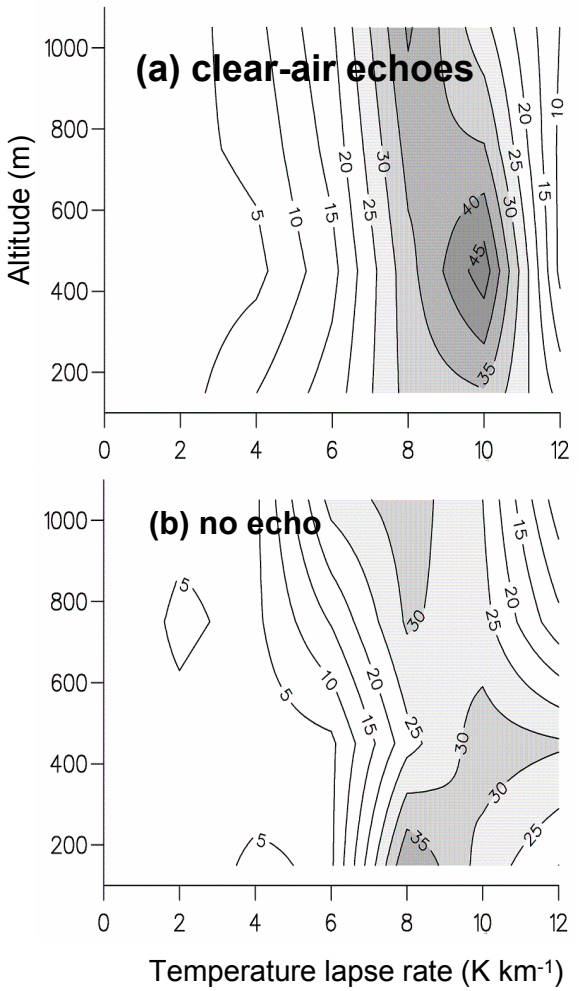

FIG. 6 The vertical distribution of the relative frequencies (%) of temperature lapse rates categorized by (a) clear-air echoes and (b) no echo.